Nuclear Instruments and Methods in Physics Research B 119 (1996) 108-114

NIM B
Beam Interactions with Materials & Atoms

ELSEVIER

X-ray generation produced by relativistic electrons in compound "multifoil structure + crystal" targets

M.Yu. Andreyashkin [a], V.V. Kaplin [a,*], A.P. Potylitsin [a], S.R. Uglov [a], V.N. Zabaev [a], K. Aramitsu [b], I. Endo [b], K. Goto [b], T. Horiguchi [b], T. Kobayashi [b], Y. Takashima [b], M. Muto [c], K. Yoshida [c], H. Nitta [d]

[a] *Nuclear Physics Institute, Tomsk Polytechnic University, Tomsk 634050, Russian Federation*
[b] *Faculty of Science, Hiroshima University, Higashi-Hiroshima 724, Japan*
[c] *Institute of Nuclear Study, University of Tokyo, Tanashi 188, Japan*
[d] *Physics Department, Tokyo Gakugei University, Koganei 184, Japan*

Received 10 November 1995; revised form received 23 April 1996

Abstract

Novel concepts of X-ray production by relativistic electrons in stratified targets are developed. It is shown that by transmitting an electron beam through a compound target, consisting of a periodic multifoil structure and a crystal, it is possible to obtain the intense, tunable, quasi-monochromatic X-rays, emitting at large (Bragg) angles with respect to the electron beam axis due to the diffraction on the crystal of resonance transition radiation, previously generated in the multilayered structure. The first results of experimental investigation of this effect for 900 MeV electrons, transmitting through the periodic stack of 10 Mylar foils and pyrolytic graphite crystal, are presented. The obtained results show that, by using of the combined radiator, it is possible to produce much more intense X-rays than parametric X-ray radiation, emitting by relativistic electrons due to the diffraction of virtual photons of electron eigenfield during the electron passage through the crystal.

1. Introduction

In the last years, the novel sources of intense, monochromatic, directed, tunable X-rays produced by electron beams, passing through matter, are intensively investigated. The radiation processes of relativistic electrons in periodic media, such as both X-ray transition radiation (TR) generating in the multilayered target and parametric X-ray radiation (PXR) emitting from the crystals, show the most promises as the possible effective sources for some practical applications [1,2].

The photon yield of X-ray TR emitting from a vacuum-material interface due to the refraction of the virtual photons of relativistic electron eigenfield [3] is not so large, about 0.0036 photons per electron in the photon energy range $E_\gamma = (0.1\text{–}1)\hbar\omega_{p_1}\gamma$, where ω_{p_1} is the material–plasma frequency, γ is the relativistic factor of electrons. But the photon yield of resonance X-ray TR (RTR), generated in the multilayered radiators consisted of a large number M of thin foils separated from each other, is much greater and may be about a few photons per electron for a few hundreds of foils. An RTR spectrum width is about 30–50%, depending on the absorption properties of foil material. RTR photons are emitted near an electron-beam direction into an annular-structure distribution with the angular radii of the rings of intensity of about a few γ^{-1}, depending on the parameters of the radiator stack. Due to the interference of TR emitted from the foil surfaces, the RTR spectral line for a certain emission direction θ has the bandwidth proportional to M^{-1} and spectral-angular intensity proportional to M^2. For example, in the case of 30 Mylar foil target and 900 MeV electrons, the spectral-angular intensity of 20 keV photons may be about 10^5 photons/electron/keV/ster for the emission angle $\theta = \gamma^{-1}$. The RTR characteristics depend on both the electron energy, the radiator parameters, and X-ray beam collimation. It is clear that RTR generated in a thick enough stack of thin foils may be used as an intense, tunable X-ray source for the some applications.

Parametric X-ray radiation (PXR) is generated by relativistic electrons passing through a single crystal [3]. PXR is associated with diffraction conversion of virtual photons of electron eigenfield into the real photons. Therefore, PXR is emitted at large (Bragg) angles with respect to the electron-beam axis, PXR spectrum shows the narrow peaks at photon

* Corresponding author.

PII S0168-583X(96)00315-1

energies defined by Bragg condition, and the positions of these spectral peaks do not depend on the electron energy. At high energy of electrons, the widths of PXR angular distribution and spectrum are mainly defined by the ratio of ω_p/ω and may be about a few γ^{-1} and a few percent, respectively. Very sharp spectral line is emitted at a certain direction into the radiation cone. Spectral-angular intensity of PXR is very high, but the photon yield is not so large as RTR one, about 10^{-5} photons per electron. The bandwidth of PXR spectrum may be decreased by collimating of the produced X-ray beam. Spectral peak positions may be changed by crystal tilting or by replacing of a collimator into PXR cone.

New concept of an intense X-ray source, produced by an electron beam in a stratified material and based on diffracted RTR (DRTR) of the relativistic electrons passing through the compound target consisting of a multilayered structure and a crystal, has been proposed in Ref. [4]. According to this concept, the multilayered structure, placed before the crystal, stands duty as a good tool for preliminary preparation of primary X-ray beam with the best characteristics for the most effective its diffraction on the crystal in order to obtain the intense, monochromatic X-rays. One expects that DRTR will unite all useful properties of both RTR and PXR, such as the high spectral-angular intensity, directionality, the large emission angles, tunability, the high degree of polarization.

One should note that, as it was shown by Caticha [5], the role of "transition diffracted radiation" mode in X-ray radiation of electrons crossing of a crystal surface could be as important as PXR. But these modes have not yet been distinguished, although, there are a lot of experimental works concerning of X-ray generation in the crystals under Bragg conditions.

2. Theoretical consideration

The differential intensity of RTR photons emitted from a multifoil target can be written as [6]

$$\frac{d^2N}{d\omega\, d\Omega} = F_1F_2F_3. \tag{1}$$

The factor F_1 corresponds to the differential intensity of TR photons generated at a single surface. The factor F_2 determines the coherent addition of TR generated at the two surfaces of a single foil. The factor F_3 describes the coherent addition of TR produced by the multiple foils in the periodical target. These factors for small emission angles θ are given by

$$F_1 = \frac{\alpha\omega\theta^2}{16\pi^2c^2}(Z_1 - Z_2)^2, \tag{2}$$

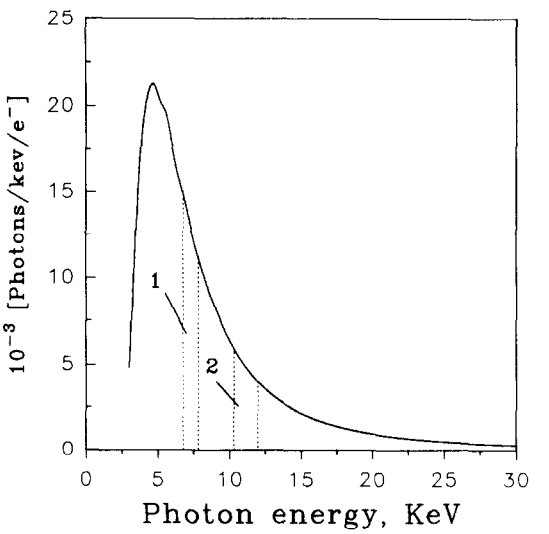

Fig. 1. Calculated spectrum of RTR generated by 900 MeV electrons in the 10 Mylar foil target (l_1 = 12 μm; l_2 = 52 μm).

$$F_2 = 1 + \exp(-\mu l_1) - 2\exp\left(-\frac{\mu l_1}{2}\right)\cos\frac{l_1\omega}{2c(\gamma^{-2} + \theta^2 + (\omega_{p1}/\omega)^2)}, \tag{3}$$

$$F_3 = \frac{1 + \exp(-M\mu l_1) - 2\exp(-M\mu l_1/2)\cos(2MX)}{1 + \exp(-\mu l_1) - 2\exp(-\mu l_1/2)\cos(2X)}, \tag{4}$$

where α is the fine-structure constant, $X = l_1/Z_1 + l_2/Z_2$; $Z_{1,2} = 4c/\omega(\gamma^{-2}+(\omega_{p1,2}/\omega)^2 + \theta^2)$ are the formation lengths of TR in the foil material and vacuum; μ is the X-ray absorption coefficient, l_1 is the foil thickness, l_2 is the foil spacing.

The spectral and angular characteristics of RTR, generated in the real multifoil target used in the experiments, were calculated by numerical integration of the expression (1). The obtained spectrum of RTR photons, emitted by 900 MeV electrons from Mylar target consisted of ten 12-μm foils with 52 μm spacings, are shown in Fig. 1. The intervals 1 and 2 show approximate widths of differential spectral lines radiating at emission angles of θ = 1.7 and 1.5 mrad. The widths of the shown intervals are $1.5\Delta E_{\gamma 0.5}$, where $\Delta E_{\gamma 0.5}$ is FWHM of differential spectral line. The value of FWHM of this line is about E_γ/M, as it follows from expression (4) describing the coherent factor F_3.

As it follows from the "resonance condition" [6],

$$\theta_r^2 = \frac{4\pi\hbar cr}{E_\gamma(l_1 + l_2)} - \gamma^{-2} - \frac{l_1}{l_1 + l_2}\left(\frac{\omega_{p1}}{\omega}\right)^2, \tag{5}$$

where $r = 1, 2, 3, \ldots$ is a harmonic number; a certain narrow range of RTR spectrum is formed by the photons radiated into the certain intervals of emission angles. From Eqs. (5) and (4), it is easy to obtain the following approximate expressions relating the angular interval $\Delta\theta$ of photon emission and the photon-energy range ΔE_γ of RTR spectrum.

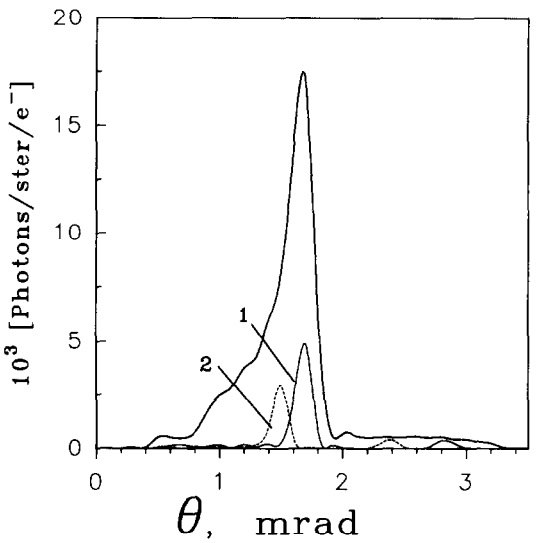

Fig. 2. Calculated angular distribution of RTR photons with energies of 5–30 keV (the upper curves). Curves 1 and 2 show the angular distributions of the photons forming RTR spectrum into energy ranges 1 and 2 (see Fig. 1).

If $\Delta E_\gamma \gg E_\gamma/M$:

$$\Delta\theta_r = \frac{\theta_r(l_1+l_2)E_\gamma^3\Delta E_\gamma}{2\pi\hbar c r E_\gamma - l_1(\hbar\omega_{p_1})^2}. \tag{6}$$

If $\Delta E_\gamma \ll E_\gamma/M$:

$$\Delta\theta_r = \frac{\pi\hbar}{(l_1+l_2)\,E_\gamma M\theta_r}. \tag{7}$$

The calculated angular distribution of RTR photons with energies of 5–30 keV is presented in Fig. 2, the upper curve. The calculated angular distribution of RTR photons with energies of 7±0.5 keV and 11±0.8 keV are also shown in Fig. 2, curves 1 and 2, respectively. RTR photons of these groups, belonging to narrow spectral intervals 1 and 2 shown in Fig. 1, form the narrow rings of intensity pattern with the angular radii θ_R = 1.7 mrad and θ_R = 1.5 mrad, respectively. Because of the relation (5) of E_γ and θ, the crystal placed on X-ray path downstream from the multifoil target should reflects only the part of X-rays belonging to the some sections of RTR angular distribution and satisfying the Bragg condition,

$$E_{\gamma B} = \frac{\pi\hbar c n}{d\sin\theta_{0B}}, \quad n = 1,2,3,\ldots, \tag{8}$$

where θ_{0B} is the Bragg angle between direction of photon emission and crystal planes, d is the crystal plane spacing.

The crystal will reflect from the differential spectral line, having the width of about E_γ/M, the photons with energy into spectral range $\Delta E_\gamma = E_{\gamma B}\cot\theta_{0B}\Delta\theta_0$, where $\Delta\theta_0$ is the parameter characterizing an ability of the crystal to reflect the monochromatic X-rays. For an ideal crystal, this parameter is the angular width of reflectivity curve, well-known

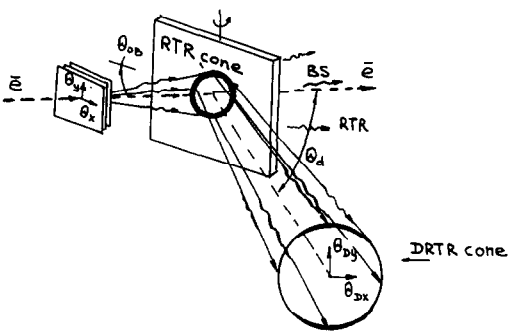

Fig. 3. Scheme of RTR photons reflection by a crystal.

as Darvin profile in X-ray diffraction theory. In the case of a real crystal, $\Delta\theta_0$ is connected with the mosaicity of the crystal, e.g. with the mean angle of a disorientation of the microcrystal blocks composing of the crystal. For a Gaussian distribution of the mosaic structure of a crystal,

$$F_M(\alpha_x;\alpha_y) = (2\pi\sigma_m^2)^{-1}\exp\left(-\frac{\alpha_x^2+\alpha_y^2}{2\sigma_m^2}\right), \tag{9}$$

where σ_m is the standard deviation of the distribution, α_x and α_y are the angular deviations of the elements of the crystal mosaic in the horizontal (the plane of diffraction) and vertical planes, respectively; the value of $\Delta\theta_0$ may be approximately determined as $\Delta\theta_0 = 6\sigma_m$. The FWHM of a differential spectral line of DRTR is about $\Delta E_{\gamma 0.5} = E_{\gamma_B}\cot\theta_{0B}(2.35\sigma_m)$.

The spectral and angular characteristics of DRTR were obtained by means of numerical calculations of the reflection of RTR photons satisfying the Bragg condition (8), by using the mosaic-structure distribution (9), and taking into account the dependence of X-ray reflectivity on the photon polarization. The calculatios were performed with taking into account of RTR photons emitted into the radiation cone $\Delta\Omega = \pi\theta^2 = 100\pi\gamma^{-2}$. The scheme of RTR reflection is shown in Fig. 3.

Fig. 4 shows the calculated angular distributions of the first order DRTR generated in the compound targets consisted of the above mentioned multifoil structure and model pyrolytic graphite crystals with different mosaicities aligned at θ_{0B} = 9.5° with respect to RTR beam axis that corresponds to Bragg energy $E_{\gamma B}$ = 11.14 keV, according to Eq. (8). Presented results show the evolution of the shape of two dimensional angular distribution of reflected X-ray photons when the crystal mosaicity increases from σ_m = 0.05 up to 3 mrad. Fig. 5a shows the angular X-ray intensity as a function of the emission angle θ_{Dx}, at a fixed angle θ_{Dy}=0. The θ_{Dy}-angular distribution of X-ray intensity at a fixed angle θ_{Dx} = 0 is presented in Fig. 5b. As it follows from Figs. 5a and 5b, curves 1 and 2, in the cases of the more perfect crystals, σ_m=0.05 and 0.3 mrad, DRTR photons are concentrated near the rings of intensity with angular radii θ_R = 1.5 mrad, which is equal in a value to the angular radius θ_R of circular distribution of RTR photons with energy

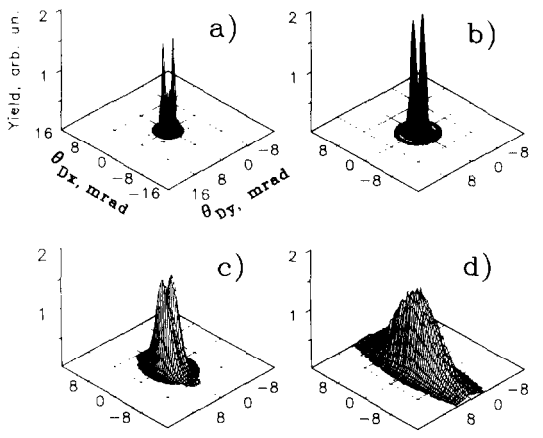

Fig. 4. Calculated angular distribution of RTR photons reflected by pyrolytic graphite crystals with mosaicity (a) $\sigma_m = 0.1$; (b) $\sigma_m = 0.3$; (c) $\sigma_m = 1.0$; and (d) $\sigma_m = 3.0$ mrad.

of about 11 keV, Fig. 2. But the intensity of X-ray photons, which are emitted near the directions with angular coordinates of $\theta_{Dy} = \pm 1.5$ mrad and $\theta_{Dx} = 0$, are the greatest due to the greater spreading of DRTR distributions in the plane of diffraction of RTR. As results, the two dimensional distributions shown in Figs. 4a and 4b demonstrate two sharp peaks of X-ray intensity in the positions which do not depend on the crystal mosaicity. The mean energies of DRTR photons forming these peaks in the angular distributions differs on the value of $\Delta E_\gamma = E_{\gamma B} \cdot \cot\theta_B \cdot 2\theta_R$. The widths of these peaks are approximately proportional to the crystal mosaicity. In the case of the crystals with sufficiently high mosaicity, $\sigma_m = 1.0$ and 3.0 mrad, the annular structure of DRTR patterns spoils due to the spreading of reflected X-ray beams because of crystal mosaicity. The θ_{Dx}-angular distributions are spread about $(\sin\theta_{0B})^{-1}$ times as much as the θ_{Dy}-ones.

The calculated profile of the spectral line of the first order DRTR versus crystal mosaicity is shown in Fig. 6. It is seen that spectral X-ray intensity and the width of spectral line increase as the crystal mosaicity increase. The full yield of DRTR photons is proportional to the crystal mosaicity. DRTR line width is mainly determined by original angular distribution of RTR photons in the case of the low mosaicity crystals. If the crystal mosaicity is large enough the line width is mainly determined by microcrystal detention σ_m. The value of spectral line width of DRTR could be approximately described by the formula $\Delta E_\gamma = E_\gamma \cot\theta_B((2\theta_R)^2 + (2.35\sigma_m)^2)^{0.5}$. By choosing of multifoil radiator parameters, the width of angular distribution of RTR photons may be decreased. Therefore, the DRTR spectral line can have more narrow width and more high spectral intensity.

We would like to note that there is a good possibility to decrease the spectral line width by means of using of curved crystal with small enough mosaicity for RTR photon reflection. The crystal curvature will be able to compensate RTR beam divergency, if $\sigma_m \ll \theta_R$. As result, DRTR spectral line

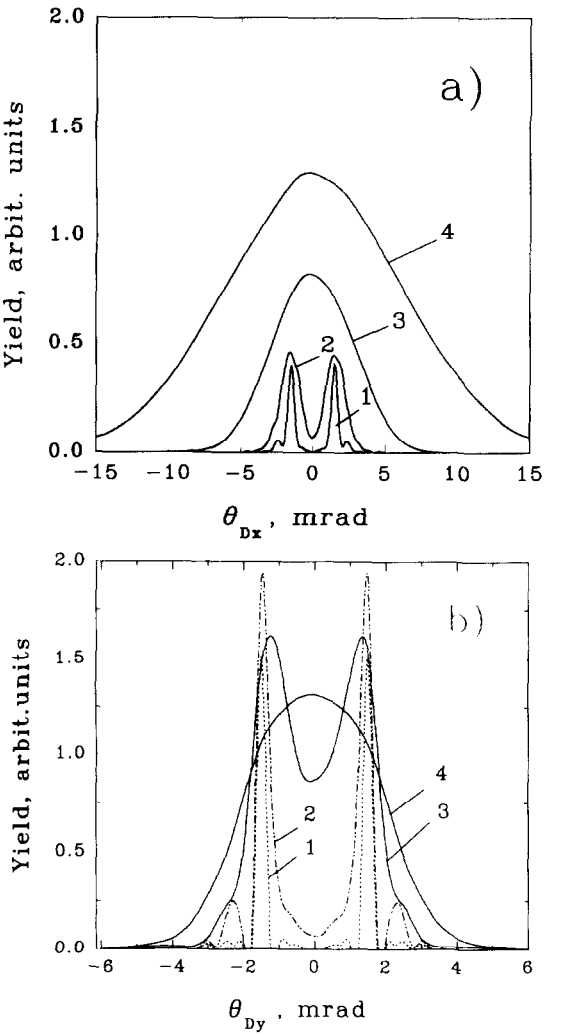

Fig. 5. (a) Diffracted RTR intensity as a function of the emission angle θ_{Dx} at fixed emission angle $\theta_{Dy} = 0$; (b) DRTR intensity as a function of θ_{Dy} at $\theta_{Dx} = 0$. Curves 1, 2, 3 and 4 correspond to the crystal mosaicity $\sigma_m = 0.1$, 0.3, 1.0 and 3.0 mrad, respectively.

width will be mainly defined by crystal mosaicity and spectral intensity may be increased in about $\theta_R/1.2\sigma_m$ times.

Note that above presented angular distributions and spectra of DRTR were calculated in arbitrary units and, therefore, give only simple illustration of the influence of crystal mosaicity on DRTR reflex and spectrum forms. But the reflectivity F_r of monochromatic and monodirected X-rays depends on crystal mosaicity. Practically, the real value of F_r are about 0.7–0.8 for perfect enough crystals and about 0.1–0.4 for mosaic crystals. One should take it into account in order to obtain exact information about the ratios of spectral or angular intensities of DRTR from different crystals. Probably, in each concrete case, it is useful to determine experimentally the value of F_r.

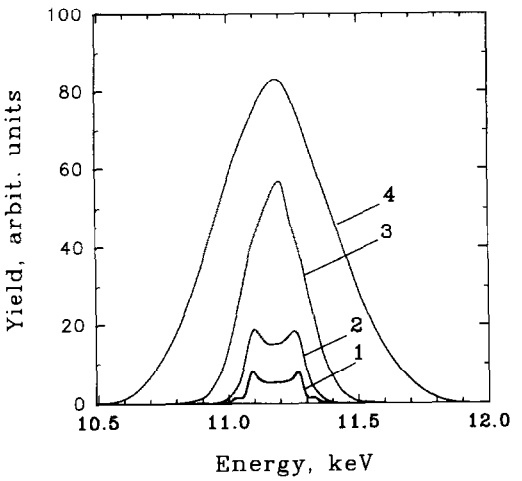

Fig. 6. DRTR spectrum versus the crystal mosaicity. Curves 1–4 correspond to σ_m = 0.1, 0.3, 1.0 and 3.0 mrad, respectively.

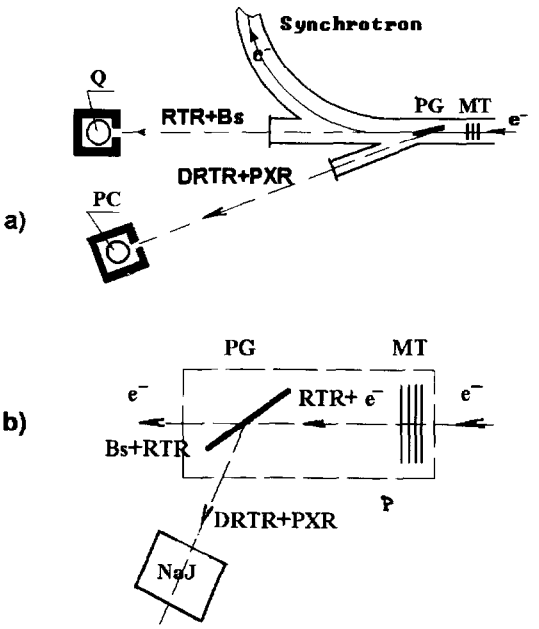

Fig. 7. Experimental arrangements at the Tomsk (a) and the Tokyo (b) synchrotrons. MT = multifoil target, PG = crystal, Q = quantometer, PC = proportional counter, P = iron plate for the mounting of MT and PG in the goniometer, NaI = scintillation spectrometer, Bs = bremsstrahlung.

3. Experimental conditions

The experimental investigation of DRTR had two stages. The first shot experiment was performed by using the internal electron beam of the electron synchrotron SIRIUS at the Nuclear Physics Institute (NPI), Tomsk, in during of the detailed investigation of PXR of 900 MeV electrons generated in a pyrolytic graphite crystal [7]. The aims of this test experiment were a testing of a multilayered target and a first observation of DRTR effect on a compound target containing the pyrolytic graphite crystal.

The scheme of the Tomsk experimental setup is shown in Fig. 7a. Electron synchrotron has a 20 ms wide flat-top with the 4 Hz repetition rate, resulting in a duty factor as high as 10%. The 900 MeV electron beam divergence was about 0.1 mrad. The crystal was placed at the internal beam in Bragg geometry. The angle between the electron beam axis and (200) crystal planes was about 9° in symmetric position. The multilayered target, consisted of 10 aluminum-coated Mylar foils with thicknesses of 12 μm and vacuum spaces of 52 μm, was placed at 3 cm distance from $10\times6\times1.5$ mm^3 pyrolytic graphite. The multilayered target could be shifted in perpendicular direction with respect to electron beam.

The photons of RTR generated in the multifoil target and then diffracted on the crystal, and PXR photons emitted from the crystal were detected by a DGR5-1 germanium semiconductor detector placed at θ_d = 18° with respect to the electron beam direction, and at a distance of 245 cm from the crystal. The detector aperture was 150 mm^2, the energy resolution at the ^{63}Zn line (8.1 keV) was about 18%.

The experimental method of the crystal aligning and the measurement of the spectral-angular characteristics of X-ray radiation are described in detail in Ref. [7].

In the test experiment at the Tomsk synchrotron, the spectrum of X-rays generated in the compound target had been measured. It was found that the photon yield from this target was about 5 times greater than that of PXR when electron beam was passed through only the crystal. It was also shown that such experimental approach to DRTR investigation is effective enough and DRTR contribution is easy extracted from the mixture spectrum due to its high intensity.

The more detailed measurements of DRTR were performed by using the extracted electron beam of the electron synchrotron at the Institute of Nuclear Study (INS), Tokyo. The external beam is more suitable for such investigations, as there are no a datum treatment problem connected with the account of incalculable peculiarity of the complicated interactions of both the electron beam with the edges of compound target and RTR with the crystal edge.

The scheme of the INS experiment is presented in Fig. 7b. The size and the angular spread of 900 MeV electron beam at the target in the horizontal and vertical directions were estimated to be 1 mm×4 mm, and 0.5 mrad×0.8 mrad, respectively, based on the beam-profile measurements by the photos. The multilayered target, namely that which was used at the NPI experiment, was mounted at a distance of 2.5 cm from 2 mm thick pyrolytic graphite crystal, which was as a 3×3 cm^2 rectangular plate with the surface orientation (200) and mosaicity σ_m = 3.27 mrad. The X-ray detector, a 1 mm thick and 25.4 mm diameter NaI(Tl) scintillation spectrometer, was placed on 142 cm distance at detection angle of θ_d = 29.6° with respect to the electron-beam axis. The detector aperture was 25.4 mm in diameter, the detection efficiency and energy resolution of the detector at

14.4 keV (^{57}Co line) were about 70% and 20%, respectively. The multilayered target and pyrolytic graphite crystal were mounted together on a goniometer, and were preliminary aligned with the aid of laser beam.

In during the INS experiment, the rocking-curve measurements of PXR and DRTR were carried out.

4. Experimental results

Fig. 8 presents the experimental spectrum of PXR generated in pyrolytic graphite crystal, curve 1, and the spectrum of X-rays emitted by the electrons transmitted through the compound target, curve 2, obtained at internal beam of Tomsk synchrotron. The shown spectra have been measured in both cases for symmetrical Bragg position, $\theta_{0B} = \theta_d/2 = 9°$, of the crystal with respect to the electron-beam axis and to the direction of X-ray observation. PXR photon spectrum shows the three brightest peaks at the photon energies of 11.2, 22.4 and 33.6 keV ($n = 1, 2, 3$ reflection orders). In the case of the compound target, when the electron beam is transmitted through the multilayered structure and then the crystal, the spectrum of X-rays emitted at $\theta = 9°$ has also three peaks at similar energies of photons. But it is clearly seen that this spectrum contains a large contribution of RTR, generated in the multilayered structure and then diffracted on the crystal. As result, the photon yield of X-ray radiation from compound target is about 5 times greater than that of pure PXR. The spectrum of DRTR component, shown in Fig. 8, curve 3, has been obtained by simple subtraction of the first experimental spectrum from the second one. The photon yield of DRTR is much greater than that of PXR. The ratio of DRTR harmonics to PXR ones, obtained with taking into account the detector resolution, is about 4.3, 3.14 and 1.85, for $n = 1, 2$ and 3, respectively. The proportion of intensity of DRTR harmonics differs from the proportion of intensity of PXR ones. The harmonic proportions obtained from experimental data are 1 : 0.16 : 0.025 and 1 : 0.235 : 0.05, for DRTR and PXR, respectively. It means that DRTR spectrum is more monochromatic than PXR one, because it contains the less contribution of high energy photons.

Fig. 9 presents a photon spectrum of PXR from the pyrolytic graphite crystal, curve 1, and a spectrum of X-rays from the compound target, curve 2, measured at the extracted beam of electron synchrotron of INS, Tokyo. The crystal was aligned at symmetrical Bragg position, ($\theta_B = \theta_d/2 = 14.8°$), in the both cases. The PXR spectrum exhibits three spectral orders at photon energies of about 7.2, 14.4 and 22 keV. The first order intensity is mainly suppressed by photon absorption in air on the way to the detector and in the detector window, because the absorption of the first order photons is much greater than that of other order ones. Therefore, the intensity of the first peak in PXR spectrum is less than that of the second one in contrast to Tomsk experiment, when the difference of the absorptions of the first and second order photons was not so large. The measured spectrum of X-rays from compound target, when the multifoil radiator is mounted before the crystal, showed the strong increase of photon yield in all spectral peaks. The yield enhancements are about 3.7 for the first spectral peak. Curve 3, in Fig. 9, shows the DRTR spectrum, obtained by means of subtraction of PXR spectrum from the spectrum of X-rays generated in the compound target. The comparison of DRTR and PXR spectra shows that the intensity of the first spectral peak of DRTR is far greater than that of PXR.

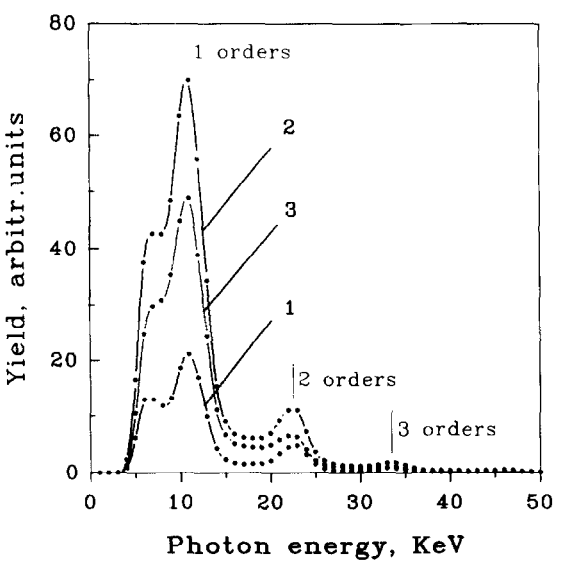

Fig. 8. Measured spectra of PXR from a pyrolytic graphite crystal, curve 1, and X-rays from a compound target, curve 2, generated by 900 MeV electrons of the internal beam of the Tomsk synchrotron. Curve 3 is the DRTR spectrum.

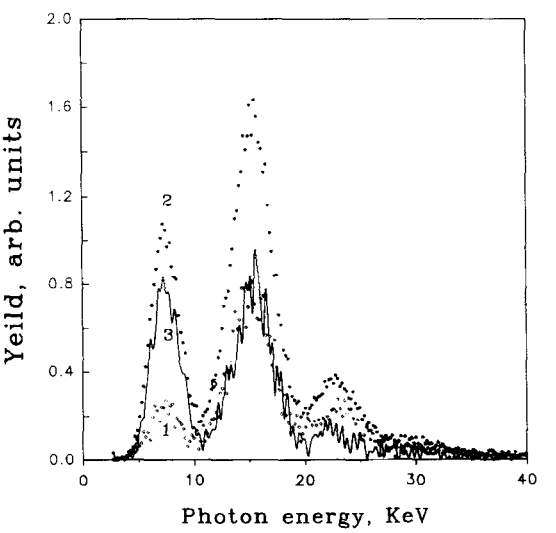

Fig. 9. Experimental spectra of PXR from a pyrolytic graphite crystal, curve 1, and X-rays from a compound target, curve 2, obtained by using the extracted 900 MeV electron beam of the Tokyo synchrotron.

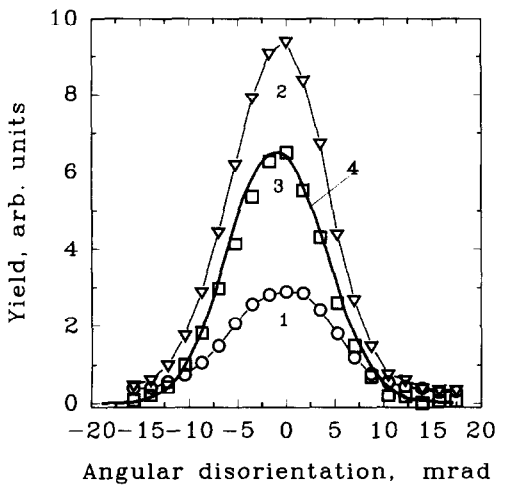

Fig. 10. Orientation dependencies of PXR from the crystal, curve 1, and X-rays from a compound target, curve 2, measured at the extracted beam of the Tokyo synchrotron. Curve 3 shows the orientation dependence of DRTR. Curve 4 is the calculated orientation dependence of DRTR.

DRTR harmonic proportion is also essentially different from PXR harmonic one.

Fig. 10 shows the orientation dependencies of the first-order yields of PXR, curve 1, and X-rays from compound target, curve 2. To obtain these curves, the corresponding spectra were measured for the various orientations of the crystal or the compound target in horizontal plane and the photon yields in the spectral region of 5.0–13.2 keV were determined. The curve 3, in Fig. 10, obtained by a subtraction of PXR data from the data measured for compound target, shows the orientation dependence of DRTR. Both orientation dependencies are the narrow, slightly asymmetrical maxima without any peculiarities. The FWHM of DRTR maximum is about 1.2 times less than that of PXR one. The obtained curve 3 gives some insight into the angular distribution of DRTR photons. It is clear that DRTR is the narrow-shaped kind of X-ray radiation as well as PXR. DRTR photons emitted about Bragg direction, into narrow cone with apex angle which depends from both the crystal mosaicity and angular characteristics of RTR, as it was shown above by theoretical calculations.

Curve 4, in Fig. 10, shows the calculated orientation dependence of the first order DRTR obtained with taking into account the detector aperture, the electron-beam size and divergence. It is seen that the profiles of theoretical and experimental curves are in a good agreement.

5. Conclusion

The above-described experimental results have shown that by transmitting of a relativistic electron beam through a compound radiator, consisting of a multifoil stack and a crystal, it is possible to effectively produce tunable, intense, quasi-monochromatic X-rays, emitting due to the diffraction on the crystal of RTR previously generated in the stack of thin foils installed before the crystal. Diffracted RTR is emitted similar to PXR at large angles with respect to the electron beam direction. The experiments have shown that, even with not so large number of thin foils composing the multilayered target, DRTR is much more brighter than PXR generated in one crystal. It is clear that, using compound radiator containing a thick multilayered structure having a few hundreds of thin foils, it is possible to make very intense X-ray source useful for a some applications. The X-ray beam produced by such source will have good enough characteristics in order that to be used for a some purposes without any additional refining.

Probably, as reflecting element of compound target, one can use instead of crystal such devices as X-ray mirrors or diffraction gratings. It is also possible to unite the processes of RTR generation and diffraction by mean of designing of periodic target consisting of a few thin crystals or a few X-ray mirrors mutually aligned respect to each other. Such kind of multicrystal or multi-X-ray mirror periodic radiators is a logical development of the idea about compound target for the large angle X-ray generation. In this case, the stack of thin crystals or X-ray mirrors is at the same time as RTR radiator and as a compound element reflecting X-rays. X-ray photons generated on the surfaces of such periodic radiators will be reflected by all following crystals or X-ray mirrors. Thus, the moving on such kind of stratified targets, more complex than that used before, may be very perspective for designing of novel X-ray sources with the best characteristics. Recently, it was shown in the experiment [8] carried out at the Tokyo synchrotron that multicrystal target gave far more intense monochromatic X-rays than PXR from continuous crystal with equivalent thickness.

References

[1] M. Moran and P.J. Ebert, Nucl. Instr. and Meth. A 242 (1986) 355.
[2] R.B. Fiorito et al., Nucl. Instr. and Meth. B 79 (1993) 758.
[3] G. Garibian and J. Shee, Transition X-Ray Radiation (Akad. Nauk Armenii, Yerevan, 1983).
[4] M.Yu. Andreyashkin, V.V. Kaplin, A.P. Potylitsin, V.N. Zabaev, S.R. Uglov, I. Endo and K. Yoshida, Proc. Int. Symp. on Rad. of Relat. Elect. in Periodical Structures, Tomsk (1993) 86.
[5] A. Caticha, Phys. Rev. A 40 (1989) 8, 4322.
[6] M.L. Ter-Mikaelian. High Energy Electromagnetic Processes in Condensed Media (Wiley, New York, 1972).
[7] K.Yu. Amosov, M.Yu. Andreyashkin, V.A. Versilov, I.E. Vnukov, V.N. Zabaev, B.N. Kalinin, V.V. Kaplin, D.V. Kustov, G.A. Naumenko, Yu.L. Pivovarov, A.P. Potylitsyn, E.I. Rozum, S.R. Uglov and M. Moran, Pis'ma Zh. Eksp. Teor. Fiz. 60 (1994) No. 7, 505; JETP Lett. 60 (1994) No. 7, 518.
[8] K. Aramitsu et al., Hiroshima University Preprint HUPD-9513, Hiroshima (1995).